Available online at www.sciencedirect.com
ScienceDirect
Thermochimica Acta 458 (2007) 23–33
thermochimica acta
www.elsevier.com/locate/tca

Cell-, biovolume- and biosurface-specific energy fluxes through marine picoplankton as a function of the assemblage size structure

Vladimir S. Mukhanov [a,*], Olga G. Naidanova [a], Olga A. Lopukhina [a], Richard B. Kemp [b]

[a] *Institute of Biology of the Southern Seas, 2 Nakhimov ave., Sevastopol 99011, Ukraine*
[b] *Institute of Biological Sciences, University of Wales, Aberystwyth, Wales SY23 3DA, UK*

Available online 6 March 2007

Abstract

The heat production of natural heterotrophic picoplankton collected in Sevastopol Bay (the Black Sea) and its long-term (from 1 to 105 days) enrichment batch-culture isolated from the same site was measured by isothermal microcalorimetry. Over the period of senescence of the culture, cell miniaturisation took place, with the average cell volume decreasing from 1.09 ± 0.15 (95% CI) to $0.18 \pm 0.02\ \mu m^3$. For the same time period, the heat fluxes decreased from 45 ± 3 fW per cell, 56 ± 13 fW μm^{-3} and 10 ± 3 fW μm^{-2} to 0.5 ± 0.2 fW per cell, 2.1 ± 1.1 fW μm^{-3} and 0.2 ± 0.1 fW μm^{-2}, thus providing evidence of the positive dependence of the fluxes on the cell size ($r^2 = 0.45$, $n = 68$). In the natural assemblage, biovolume- and biosurface-specific heat fluxes insignificantly ($r^2 = 0.19$ and 0.12, respectively; $n = 25$) increased with decreasing average cell size from 0.75 ± 0.12 to $0.13 \pm 0.04\ \mu m^3$, to give indirect evidence that at least a part of the ultramicrobacterial pool are cells with high volume-specific metabolic rate. The maximum biosurface-specific metabolic rate measured for the natural bacteria proved to be close to those averaged for actively growing aquatic protozoans at 1.3×10^{-15} mol O_2 $\mu m^{-2}\ h^{-1}$ (equivalent to 2×10^{-13} W μm^{-2} for purely aerobic metabolism), as calculated from published data. The latter does not depend on the cell volume ($r^2 < 0.001$, $n = 58$) over the size range from 10^2 (smallest flagellates) to $10^8\ \mu m^3$ (largest sarcodines), supplying illustrative evidence for Rubner's law. Marine bacteria ($10^{-1}\ \mu m^3$) appear to fit this law and extend its scale by 2 orders of magnitude.

Keywords: Picoplankton; Metabolic rate; Heat flow; Microcalorimetry; Size distribution; Long-term stationary phase

1. Introduction

The annual production of prokaryotic microorganisms in the world's oceans that are involved in the microbial food web amounts to about 10^{29} cells, equivalent to 10–20 Gt carbon per year [1]. This is about half the total annual primary production in the oceans of up to 50 Gt C [2]. Heterotrophic picoplankton form the so-called *microbial loop* [3] in which they (i) degrade dissolved and particulate organic matter pools supplied in the detrital food chain, and (ii) re-mineralize organic matter providing inorganic nutrients for the primary producing photoautotrophs. Primary and secondary production derived from the picoplankton are utilized by bacterivorous and herbivorous protists (mostly ciliates and nanoflagellates) [4,5] to complete the microbial loop and couple the microbial food web with the upper levels of the trophic pyramid. Thus, picoplankton mediate the material flows through the aquatic microbial food web and play a central role in the global biogeochemical cycles of carbon and nutrients.

The driving force for the material flows in all living systems and, thus, in aquatic ecosystems is the Gibbs energy ($-\Delta G$) from catabolic processes [6]. Although without this force the flows cease, current knowledge of how material and energy flows are coupled to each other at the community and ecosystem levels is still scarce. There is an acute shortage of direct data on the energy flows through pelagic microbial communities compared with the data available on their mass variables like biomass/biovolume, production, specific growth rate, grazing mortality, etc. For the better understanding of how the pelagic microbial food web functions, therefore, it is crucial to know (i) the sources, pathways and sinks of energy in it; (ii) the rates at which the energy is transferred through the web compartments; and, finally, (iii) the feedback-control mechanisms between the energy and matter flows and stocks. This study is focused just

* Corresponding author. Tel.: +380 692 542484; fax: +380 692 557813.
E-mail address: vmukhanov@mail.ru (V.S. Mukhanov).

0040-6031/$ – see front matter © 2007 Elsevier B.V. All rights reserved.
doi:10.1016/j.tca.2007.02.024

on some important aspects of the latter two problems. In particular, we measured directly the energy flow through a marine picoplankton community and combined the results with conventional microscopy in order to explore the dependence of energy fluxes (per cell, biovolume and biosurface) on the size structure of the community.

The methodology generally used for measuring the energy flows in the components of the microplankton is far from being perfect. First, it is difficult to separate the microbial population of interest from the other parts of the complex assemblage. Usually, it is a functional group or a compartment of the microbial food web, for example the photoautotrophic picoplankton (cyanobacteria, eucaryotic picoalgae as primary producers) or the heterotrophic nanoplankton (nanoflagellates grazing on bacteria), etc. Microfiltration is widely used in the field of aquatic microbial ecology but it is not always narrow enough in scale (e.g. to differentiate between heterotrophs and photoautotrophs in the same size class) or sufficiently delicate in application (e.g. to separate fragile small flagellates and large phytoplankton without destroying/damaging them [7,8]) to solve this problem perfectly. Nevertheless, the method can be efficient for separating and concentrating planktonic bacteria for further physiological experiments [9–11].

To the present time, indirect methods mostly have been applied to measure the energy flow through an aquatic microbial community, with unavoidable speculation having to be made to interpret the results. For example, the use of the respirometric approach is based on the assumptions that: (i) catabolism is totally aerobic; and (ii) in order to obtain thermodynamic information, the oxygen consumed in respiration is equivalent to the heat produced as a measure of energy flow by a factor called the oxycaloric equivalent [12] which is constant for the combustion of a given substrate. Given that the enthalpy change of anabolism equals zero [13,14], O_2 uptake by an aquatic ecosystem and its catabolism are considered synonymous with the ecosystem energy flow. However, it is dangerous to define respiration as the only catabolic process in the water column under the relatively adverse *in situ* conditions that occur particularly deep in the photic zone and beyond and, hence, to equate indirect calorimetry with the direct one. Another source of error is that there may be oxidative chemical processes in aquatic environments, which would be manifest as oxygen uptake (e.g. [15,16]). In this case, respiration would not be the only oxygen-consuming process in the water column.

The microcalorimetric approach which was used in this study is ideal for bridging the knowledge and methodological gaps mentioned above because it: (i) provides direct information on the kinetics of heat (i.e. energy) dissipation in a biological system, and measures the rate of integral metabolism involving both aerobic and anaerobic processes; and (ii) was recently adapted and applied to measuring the metabolic rate of natural bacterioplankton in marine [9] and hypersaline [10] environments.

The viability and/or physiological status in terms of metabolic activity of single cells can be recognized using epifluorescence microscopy and a number of markers, like propidium iodide (PI) for staining only dead cells [17] and 5-cyano-2,3-ditoyl tetrazolium chloride (CTC) which is reduced in respiring cells into water-insoluble red formazan crystals [18,19]. However, it is still technically impossible to measure the metabolic rate of an individual bacterial cell in terms of oxygen uptake or heat flow. For this reason, cell- and volume-specific metabolic rates are commonly averaged for the total cell population. In this study, we followed this conventional way with no differentiation between dead/alive and active/dormant cells. In addition, we did not correct the heat flows measured experimentally at 20 °C to the *in situ* temperatures because our objective was not to study a particular picoplankton community at a specific location but rather to search for a fundamental link between the community energetics and its structure in natural conditions of nutrient supply and in enriched nutrient levels that can affect the dynamics of the relationship. In order to relate the energetics to the morphometric characteristics of the community it was essential to cover as wide a cell size scale as possible and this was achieved in two ways. In one, samples were collected from a mesocosm, that is a circulating water reservoir with seawater, in which the average cell size of the bacteria was larger than in the sea. In the other, we employed nutrient-enriched heterotrophic picoplankton with cell sizes ranging to a maximum of 2 μm^3.

The use of the enrichment culture gave an opportunity to explore the energetics of senescent bacteria by monitoring their cell size reduction (miniaturisation) and changes in metabolic rate over a long-term (15-week) stationary phase. Interest in the phenomenon of bacterial senescence has greatly increased in the last few years [20,21] because of a growing understanding that in a long-term batch culture, the cells undergo morphological, physiological and gene-expression changes similar to those observed in natural environments [21]. The most exciting finding was an expression of the so-called 'growth advantage in stationary phase' (GASP) phenotype by mutant cells in a long-term batch monospecific culture, which resulted in enormously increased genetic diversity of the bacteria and their ability to utilize additional growth substrates [22,23]. It was felt that looking at the energy flows in enrichment cultures may give clues to the as yet poorly understood physiology of bacterial senescence.

2. Experimental

2.1. Sample preparation

The surface water samples were collected at one particular sampling station in Sevastopol Bay (the Black Sea, Ukraine) at different seasons from July 2000 to May 2002. Both natural, that is unaltered samples, and culture-enriched picoplankton were used in the microcalorimetric experiments.

Enrichment of heterotrophic picoplankton was achieved by firstly screening 50-ml sub-samples of the coastal seawater with 3 μm pore size nitrocellulose membranes (Sartorius #SM113 02-047) to remove micro- and nanoplankton and then inoculating the <3-μm filtrates into 250 ml of peptone water containing 1% (w/v) bactopeptone (Spofa a.s., Prague, Czech Republic), 0.5% NaCl, 0.01% KNO_3 and 0.2% $NaHCO_3$ prepared in sterile dis-

tilled water. Over the study period, seven enrichment cultures were set up, incubated in 500 ml flasks at room temperature in the dark, and observed for up to 15 weeks for their aging and cell miniaturization.

Picoplankton samples were additionally taken from a recirculating (0.25 $m^3\,h^{-1}$) 7-m^3 aquarium tank that constituted a 'mesocosm', which was incorporated into a system of interconnected 3- and 7-m^3 aquaria and a 100-m^3 accumulator tank supplied with seawater from Sevastopol Bay. Seawater passed through a coarse-mesh filter cartridge and was aerated by air-bubbling. Its temperature was not specially regulated so it varied somewhat with the ambient in the aquarium, though within a narrower range than that *in situ*.

Picoplankton were counted by epifluorescence microscopy using proflavin hemisulphate as the fluorochrome [24] and a Zeiss JENALUMAR-a/d microscope equipped with an HBO-202 mercury lamp and a filter set for blue light excitation (KP425 + B228/229 excitation filters, TS510 beam splitter and G247/249 barrier filter). After staining, samples were fixed with glutaraldehyde (10%, 0.1 μm prefiltered, 1% final concentration) and collected onto black-stained polycarbonate membrane filters (0.2 μm pore size, Trackpore Technology, Dubna, Russia; http://www.trackpore.ru) at low vacuum (80 mmHg). At least 200 cells and 20 fields were counted on each preparation. Photoautotrophs were identified by the autofluorescence of the photosynthetic pigments.

At least 50 bacterial cells from each sample were sized (length, diameter, cell volume and surface) using a light microscope (Biolam R-17, USSR), high magnification (1350×) and erythrosin staining according to [25]. Bacteria from seawater sub-samples preserved in 3% formaldehyde were collected onto a nitrocellulose membrane filter with the pore size of 0.2 μm (Sartorius # SM 11318-047, Germany). The membrane filter was dried and placed onto a paper filter soaked with 3% erythrosin solution in 5% phenol, and stained in a closed Petri dish for 2–3 h. The stained filter was washed several times in the same way by placing it on the surface of a paper filter moistened with distilled water for it to become a light pink colour. Then the filter was dried and put on a drop of immersion oil on a glass slide to make it transparent. It was covered by another drop of the oil and a cover-slip, and examined microscopically under immersion.

2.2. Morphometric calculations

The volume of the bacteria was calculated using the formula $V = (\pi/4)W^2(L - W/3)$, where L is cell length, and W is cell width [26,27]. The surface area of individual cells was computed as $S = \pi \times W \times L$.

Biovolume and biosurface were estimated from the data on cell abundance and dimensions, and were used together with the microcalorimetric results (see below) for calculating scalar (per unit of biovolume) and vector (per unit of biosurface) heat fluxes.

2.3. Microcalorimetry

The average rate of the bacterial assemblage metabolism was measured by the microcalorimetric method as the heat flow rate using an LKB BioActivity Monitor (BAM), Model 2277 (the successor is the Thermal Activity Monitor (TAM), Thermometric AB, Järfälla, Sweden) equipped with three independent sets of twin differential channels, one of each twin for the test material and the other as the control. All the experiments were conducted at 20 °C.

The enriched community had living biomass concentrations high enough to perform direct heat flow measurements without any concentration of the samples. The picoplankton from the natural waters and the mesocosm, on the other hand, had to be concentrated by a two-step filtration technique [9–11] to be above the detection limit of the instrument. When applying the concentration method to these assemblages, it was necessary to determine as a preliminary stage that sufficient cells were concentrated to allow calorimetric detection and to relate their morphometry to that of the enriched community.

As the first step of the trial, the seawater samples were screened as usual with a 3 μm pore size membrane (Sartorius # SM 11302-047) to remove nano- and microplankton (Fig. 1A). The 3 μm filtrate contained the so-called *picoseston* which included microorganisms as picoplankton and detrital particles. Mukhanov and Kemp [11] had shown already that the heat flow it produces is due mostly to the living component, i.e. microbial metabolism. According to the microscopical examination of microorganisms in the fraction, the concentrations of cells in taxonomic groups other than bacterioplankton,

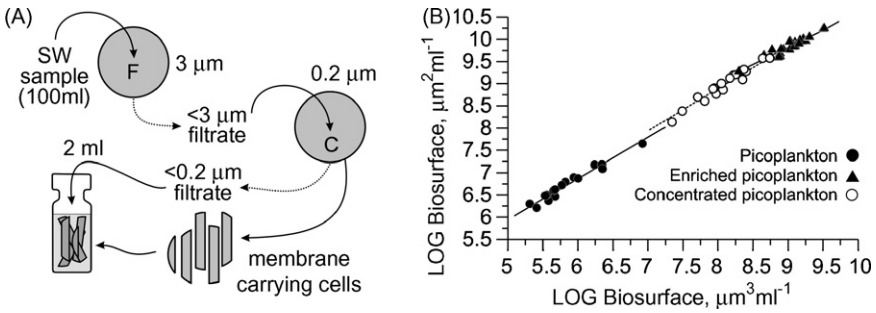

Fig. 1. Concentration of natural picoplankton prior to microcalorimetric measurements of metabolic rate. (A) Two-step filtration technique involving seawater (SW) sample fractionation (F) and concentration (C) using nitrocellulose membranes. (B) Ranges of biovolume and biosurface observed in unaltered (natural and mesocosm samples, ●), enriched (▲) and concentrated (◯) picoplankton.

including any cyanobacteria, picoalgae and small nanoplankton passing through the membrane, were too low (not more than 2% in terms of biomass) to affect the calorimetric measurements and, thereby, the heat flux calculations. For this reason, the heat flow by the picoseston was considered to be associated solely with the metabolism of the heterotrophic bacteria. Nevertheless, it was decided that all the subsequent samples must be microscopically examined to check for potential artefacts caused, for example, by a bloom of a photoautotrophic species.

As a trial of the second stage of preparing the unaltered picoplankton fraction, 100 ml sub-samples of the <3-μm filtrate were concentrated onto 0.2 μm nitrocellulose membranes (Sartorius # SM 11318-047) (Fig. 1A, membrane C). Each wet membrane (or its fragment of known area) with the concentrated cells was cut into strips to maximise exposure of the surface to the sea water and placed into a sterile measuring ampoule containing 2 ml of particle-free seawater (PFSW) from the same site. The ampoule was hermetically sealed and the bacterial heat flow was measured immediately after loading the glass ampoule with its filter membrane carrying the bacteria into the batch module of the microcalorimeter and equilibrating it to 20 °C. A 0.2 μm pore size nitrocellulose membrane (SM 11318-047) was used for preparing PFSW.

As seen in Fig. 1B, the concentration procedure resulted in a sufficient increase in the picoplankton biovolume and biosurface in the measuring ampoule to make them equal to the values observed in the enriched assemblages. Furthermore, the heat flow was above the 1 μW calorimetric detection limit. The volume of the concentrated sample (100 ml) was chosen because it was large enough to be considered representative of the *in situ* assemblage according to Kirchman's [28] sampling hierarchy and associated statistics. At the same time, it was small enough to avoid the large calorimetric measurement error associated with concentrating bacteria onto the membrane. A further methodological problem to address was the possibility that concentrating the cells on a filter caused the well-known "crowding effect" leading to depressed metabolism. Mukhanov and Kemp (in preparation) had shown that bacterial heat flow was depressed with increasing filtered volume (up to 1.5 l) and cell number (up to 10^9 cells) on and inside the nitrocellulose membrane matrix. Fig. 2 shows that, for samples taken from natural waters at different times, this resulted in a hyperbolic relationship between heat flow and the number of the concentrated bacteria. However, it was calculated that, at relatively small filtered volumes (100 ml corresponds to about 10^8 cells) the depression-associated error was minor, never exceeding 5%. As a result of all these checks on the two-step filtration technique, it was considered suitable for the current investigation.

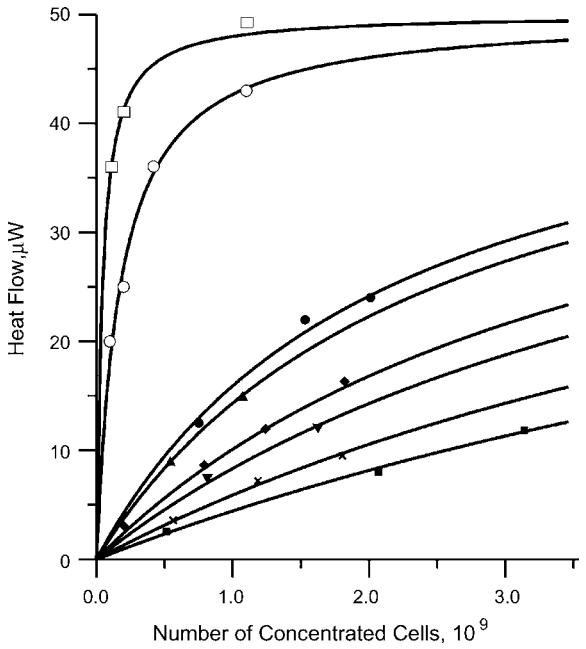

Fig. 2. The "crowding effect" represented as hyperbolic relationships between the number of the bacteria settled onto a nitrocellulose membrane and their heat production. Symbols of a given shape on a particular curve correspond to a set of parallel experiments with replicates of the same seawater sample but different concentrated volumes. Several different samples were taken from the same site (or culture) at different times and gave a range of curves. Open symbols are for the enriched assemblage, solid ones are for the concentrated ones.

3. Results

As can be seen in the inset to Fig. 3, the size spectra of the picoplankton examined in this study were chosen from all the accumulated data to give a broad range of average cell volumes from about 0.1 μm^3 (Fig. 3D) for the smallest example of the natural assemblage to more than 0.7 μm^3 (Fig. 3E) for the mesocosm and over 1.0 μm^3 (Fig. 3H) for the enriched culture. The size distribution of individual cells in all the studied systems (see spectra in Fig. 3) followed the same pattern: samples with the higher average cell size were characterized by a relatively wide size spectrum, i.e. they included both large and small cells (Fig. 3A versus D, E versus G, H versus K). At the average cell volume of 0.2 μm^3, the chosen size spectra overlapped, allowing for their comparison (see the spectra B, G and K in Fig. 3), which showed that the frequency distribution was asymmetric, with the smallest cells dominating the natural and mesocosm samples (the peaks to the left) and with the larger cells foremost in the cultures (right-side peak). It is notable that the samples with the smallest average cell size, taken from the Bay water (Fig. 3D) and the senescent culture (Fig. 3K), lost large cells completely while they never disappeared in the mesocosm, being a flow system at quasi-steady state (Fig. 3G).

The difference between the natural and enriched assemblages was in the range of variability (Fig. 4). The cultures demonstrated the wider spectrum of cell sizes with the largest volume of up to 2 μm^3 compared to about 0.9 μm^3 in the natural samples. During the culture aging, the spectrum became narrower and shifted to smaller sizes (Fig. 3H–K; Fig. 4A) as evidence of cell miniaturization. By comparing the regressions in Fig. 4A and B, it can be seen that the nature of the dependence between the cell volume and the surface was the same in all the systems, but the coefficients of variation of the average cell surface (42–46%) were lower than those of the average cell volume (58–63%).

The heat flow traces recorded for the first week of the culture aging (Fig. 5A) were bell-shaped, i.e. the same as usually observed in freshly inoculated batch bacterial cultures. This was

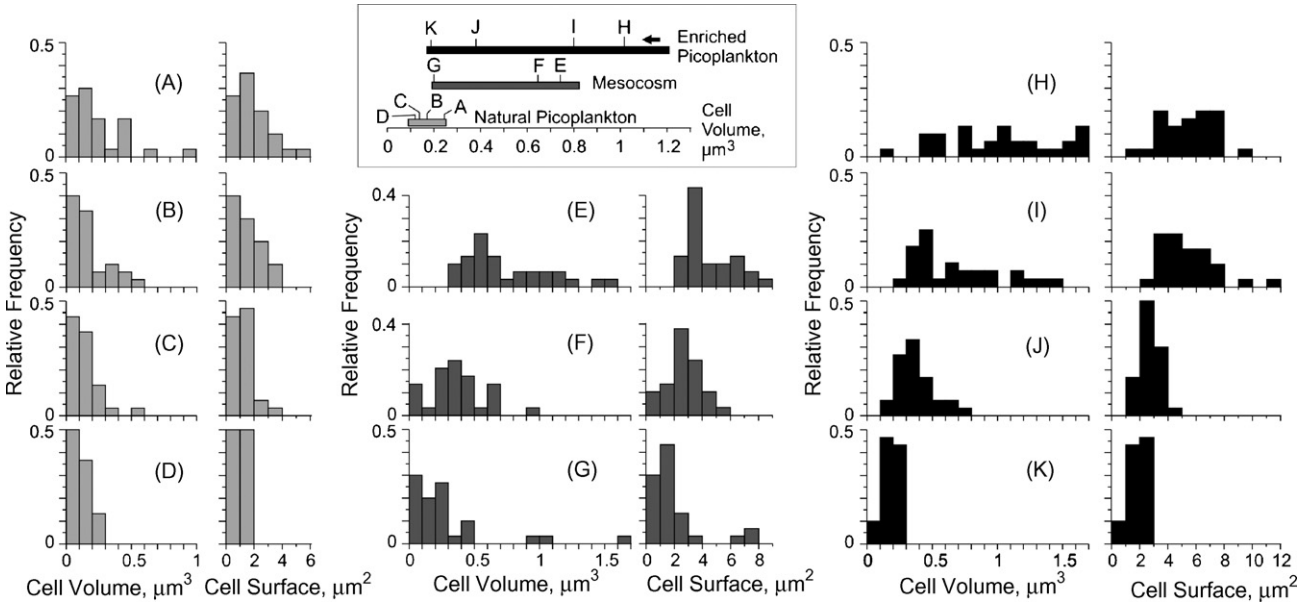

Fig. 3. The range of chosen size spectra of natural (A–D), mesocosm (E–G) and enriched (H–K) picoplankton assemblages. Letters on the inset diagram correspond to those on the plots. The arrow on the inset shows the direction of the tendency to cell miniaturization in the enrichment cultures aging for 15 weeks on their transient to a long-term stationary phase.

despite the fact that no fresh medium was added to the sample and that the latter initially was at the same cell number concentration as in the natural community. After the apparent metabolic burst, however, the heat flow dropped to extremely low levels (a few μW per ampoule, below 1 fW per cell). As can be seen in Fig. 5A, the heat flow profiles changed over the period of culture aging in that: (i) the initial heat flow, i.e. that measured at the start point of the microcalorimetric experiment, decreased; (ii) the peak height decreased; and, (iii) finally, the peak disappeared altogether.

The heat fluxes calculated at the start point of the aging experiments were roughly the same per cell (45 ± 3 (95% CI) fW per cell, averaged for 2-day cultures only, $n = 3$) and its volume (56 ± 13 fW μm^{-3}), (approximately 30 fW for the regression lines in Fig. 5B), and were 10 ± 3 fW per surface (μm^{-2}) (about 5 fW for the regression in Fig. 5B). They decreased over the 15-week culture period aging to extremely low values, 0.5 ± 0.2 fW per cell (averaged for 80–105-day cultures, $n = 6$), 2.1 ± 1.1 fW μm^{-3} and 0.2 ± 0.1 fW μm^{-2}. The 'per cell' scalar flux decreased faster than the others owing to the replacement of rods by cocci during the cell miniaturization. At the start point, the average volume of the cells was close to 1 μm^3 while at the finish of the experiment, the cell surface area of the miniaturized cells was about 1 μm^2. These are the reasons why the 'per cell' regression line joins the others, forming an inverted Z-shaped pattern (Fig. 5B).

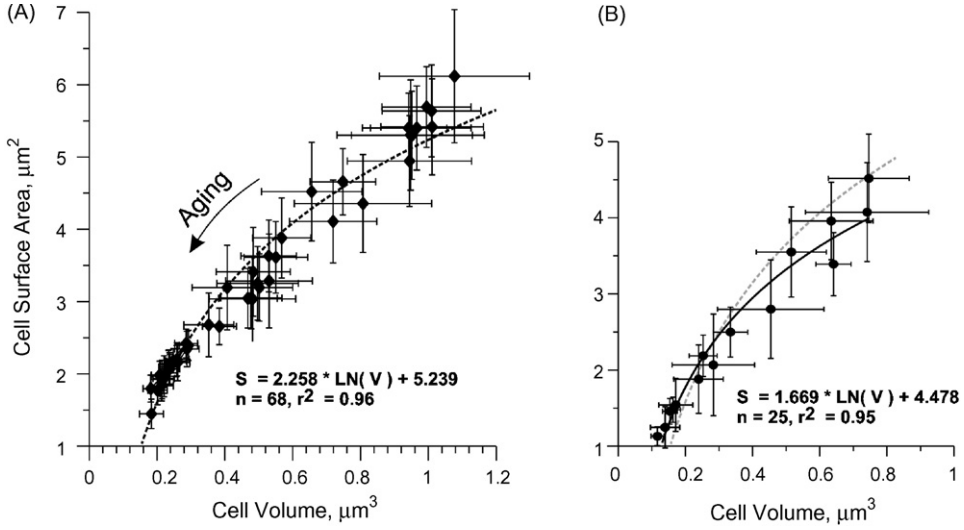

Fig. 4. Morphometry of picoplankton in the enrichment culture (A) and in both the natural and the mesocosm assemblages (B). The arrow indicates the tendency to cell miniaturization in the culture during aging for 15 weeks. The bars are 95% confidence intervals (CI). The dashed line in plot B represents the regression obtained for the enriched assemblage (plot A).

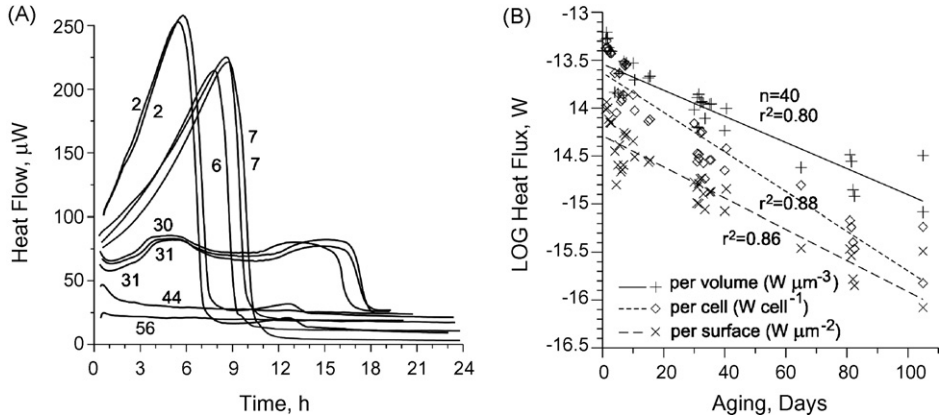

Fig. 5. Changes in the heat flow patterns (A) recorded for 2-ml samples of the cultures at different age (numbers are days) and the decrease in the energy fluxes during the process of culture aging (B). The fluxes were calculated using the cell number concentrations for the start points of the experiments.

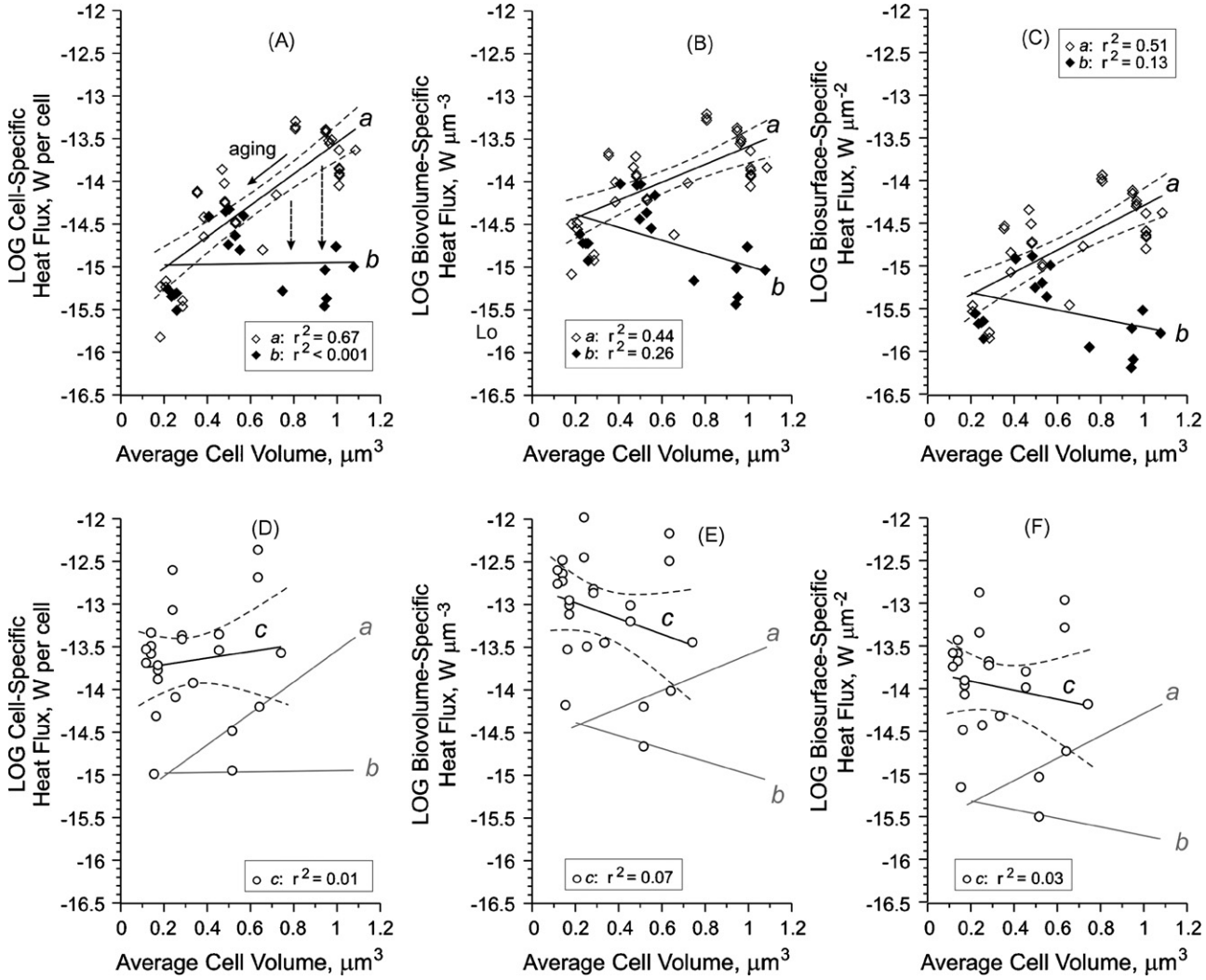

Fig. 6. Cell- (A, D), biovolume- (B, E) and biosurface-specific (C, F) heat fluxes measured in the enrichment culture (A–C; regressions *a* and *b* for the start and finish points of the microcalorimetric experiment, respectively) and the picoplankton assemblages (D–F; regression *c* is for both mesocosm and natural waters; regressions *a* and *b* from the plots A–C are reproduced for comparison). The solid arrow indicates the culture aging. Dashed arrows show the tendency for the heat flux to change over the time of the microcalorimetric experiments. Dashed curves are 95% confidence intervals.

The dependences of the energy fluxes on the average cell size in the enriched picoplankton (Fig. 6A–C) are the quintessence of the results presented in Fig. 5. The fluxes measured at the start of the experiments (Fig. 6, regression *a*) decreased with decreasing cell size while those at the finish (Fig. 6, regression *b*) either did not change (Fig. 6A) or increased with decreasing cell size (Fig. 6B and C).

The Bay and mesocosm picoplankton did not exhibit significant dependence of the fluxes on the average cell size (Fig. 6D–F, regression *c*), with the volume-specific heat flux increasing slightly ($r^2 = 0.07$) with decreasing cell size. The slope of the regressions *b* agreed closely with those of the corresponding regressions *c* but the fluxes in the culture were about 25 times lower than in the Bay and mesocosm picoplankton.

4. Discussion

When attempting to explain the data in Fig. 3, it is important to recall that the active bacterial growth occurring after enrichment of seawater with dissolved organic nutrients is commonly accompanied by rapid changes in the structure of the bacterioplankton community in terms of shifts towards the predominance of a few typical, culturable genera [29,30]. The process can proceed without activating the pool of what are regarded as 'dormant cells' [29]. This can explain why small cells remained in the culture over the period of active growth, keeping the wide size spectrum illustrated in Fig. 3H and I. Over the long-term stationary phase, the spectrum became narrower (see Fig. 3J and K) owing to cell miniaturization as previously reported [20,31] and, probably, the lysis of larger cells. Finally, the aged culture contained only small cells, which potentially could have different origins: (i) small bacteria (*oligobacteria* [32], see below) remaining in the culture from the first days after the enrichment and retaining their small size; and (ii) large copiotrophic bacteria which actively grew after the culture enrichment but reduced in size on depletion of the nutrient resources, i.e. they had become starvation forms [33]. The fate of the first population was unknown—either they remained in the culture for a long time or they lysed and were substituted by the second population. Differentiation between the contributions of the above populations to the total bacterial abundance, biomass and activity in the enrichment culture was not performed in this study. However, such analysis could increase our general understanding of the microbial processes occurring in the long-term, stationary phase enrichment cultures of bacterioplankton [34].

In standard monospecific laboratory cultures, a substantial number of viable cells in the population (up to 10^6 cells ml^{-1} [35]) survived for a very long time, even longer than for 5 years [35], in a long-term stationary phase (see review [21]). No additional nutrients were required for sustaining the cultures, but sterile distilled water had to be supplied to maintain the initial volume and the osmolarity of the medium [35]. The key to such 'immortality' was shown to be mostly the genetic alterations occurring in the majority of cells and expressed as the GASP phenotype [23,35,36]. It appears that GASP mutations enable bacteria to catabolise amino acids as additional substrates which earlier were inaccessible as sources of carbon and energy [22,23]. As a result, monospecific batch cultures entering a stationary phase possess an enormous genetic and consequent morphological diversity to fit it for survival. Such a strategy must be available to the species composing the picoplankton community as a multispecies system, thus making the structural diversity of the enriched community from natural sources enormously high.

The remarkable decrease in the bacterial heat fluxes over 15 weeks to about 1–3% of the values measured on the second day after the sample enrichment (Fig. 5B) is in accordance with previous findings [37–41], namely that reduced respiration and low endogenous metabolism are the result of sparse nutrient conditions. What was remarkable is the heat bursts observed every time the culture sub-samples were loaded into the microcalorimeter (Fig. 5A, the curves for days 2, 6 and 7). The cells were probably triggered to activate their metabolism by sample manipulation in the form of mechanical disturbance whilst obtaining the sub-sample from the culture and pouring it into the measuring ampoule, together with a minor change in temperature on transferring the sub-sample from the culture room to the microcalorimeter. We suggest that the abrupt drop in heat flow which followed the burst was a penalty for the wrong timing of cell growth. Thus, the responses of younger and older cultures were different, and the flux/average cell size relationships of the culture at the end of the measurement period were similar to those in the unaltered natural community (see Fig. 6) in that the regression lines *b* are parallel to *c*, with the difference in the values of about 1.5 orders of magnitude. We are unable to interpret the result at this stage—more detailed physiological studies are required to clarify this matter.

The slopes of the regression lines in Fig. 6D and E conformed to known, fundamental relationships, called Kleiber's rule [42,43], originally formulated for those between animal energetics and their size: that is, in terms of their metabolism, smaller bacteria gave less heat flux on a "per cell" basis (Fig. 6D) but their volume-specific heat flux was higher than in larger cells (Fig. 6E). The regressions obtained for the data, however, were statistically insignificant. In this context, it is worth recalling that Makarieva and Gorshkov [44] showed there was no significant relationship between mass-specific metabolic rate and cell mass for 80 species of prokaryotes ranging physiologically from endogenous to growth metabolism and in mean cell volume from 1.4×10^{-2} to 2×10^4 μm^3. However, another possible explanation of the lack of size dependence in the samples of the picoplankton community is the structural complexity of the studied systems, for instance in terms of multispecies and different cell morphotypes, while also having cells in different physiological states. Consequently, a conceptual approach different from that typically applied to physiological experiments with synchronized cultures of microbial monospecies has to be applied to analyse such results.

The adopted approach required, first, that the fluxes presented in Figs. 4–6 are interpreted in terms of the functional 'physiology' of the whole community rather than of single cells, meaning that the terms 'cell volume' and 'cell surface' need to be changed to 'biovolume' and 'biosurface' because the latter characterize a supracellular system. Secondly, it must be kept in mind that the

energy fluxes were determined as *averaged* rates because the viability and the physiological status of individual cells were ignored and, as a result, the *total* abundance, biovolume and biosurface were used in the calculations. Such an approach is common in field studies of microplankton with the only difference that the cell-specific metabolic rate is measured in terms of the rate of respiration (e.g. [45]). As a community-level variable, the *average cell size* showed the predominance of a given size of cells in the sample but it did not describe the whole size spectrum. It meant of course that if the average cell size was small (i.e. abundance of smaller cells was large), the sample still could contain big bacterial cells (as was the case in the mesocosm) whose contribution to the total energetics of the sample was likely to be considerable because of their large biomass.

After taking the above stipulations into account, the conclusion drawn from Fig. 6 in its strict formulation is that the average energy fluxes per cell, the unit of the community biovolume and the unit of its biosurface were independent of the size structure of the community. If it is concluded that the energetics of individual cells forming the assemblage depends on cell size, the question then arises as to how the cell size-dependent energetics sums up to produce size-independent community-level energy fluxes. It is proposed that the key to this apparent contradiction may lie in understanding how alive/dead and metabolically active/inactive cells are distributed among the different size classes of planktonic bacteria.

The smallest bacteria (the so-called ultramicrobacteria, UMB) morphometrically are "femtobacterioplankton", in the plankton *femto*fraction, <0.2 μm, according to [46]. They dominate the bacterioplankton assemblage in terms of abundance, far exceeding the numbers of copiotrophic large bacteria. The population of small cells consist of the obligate oligotrophic UMB whose cell volume ranges between about 0.014 and 0.07 μm^3 [47,48] and the similarly sized starvation forms of the copiotrophs. Since there is mixed population of small bacteria, perhaps it is not surprising that published data on the physiological status of them are highly contradictory (see reviews [33,49]), providing evidence that they either are dormant [50] or have highly active metabolic activity [51]. Indeed, both the points can be true depending on the nature of the cells under consideration. The major distinction is that starvation forms are a temporary response to stress and are able to recover and increase their cell volumes under favourable conditions [29,52]. On the other hand, some of the UMB are well adapted to low nutrient, oligotrophic environments and do not increase in average cell size on exposure to multiple nutrient media [32,51,53]. The volume-specific metabolic rates of both the groups are different in that the small starving bacteria in the UMB, thought to originate from copiotrophs, are dormant according to Stevenson's hypothesis [54] and the results supporting it (e.g. [50]) whereas the oligotrophic UMB are growing cells [55,56], i.e. they must be metabolically active. Moreover, the volume-specific metabolic rate of the latter is supposed [51,57,58] to be even higher than those of the so-called 'normal' bacteria. Our results provided indirect evidence for the idea that at least a part of the UMB are metabolically active because it follows from Fig. 6E that the samples with low average cell size (i.e. the predominant small bacteria) did not demonstrate lower heat flow rates compared to those with relatively high average cell size. In order to know how the metabolic activity of the assemblage is distributed among individual cells and, finally, to explain the lack of the dependence seen in Fig. 6E, it will be necessary to determine precisely the ratios between the three sub-populations of dead, 'alive but dormant' (miniaturised copiotrophs) and 'alive and active' cells (possibly oligotrophs) in a particular water sample—a difficult task.

The fraction of active, respiring bacterial cells positively identified by staining with CTC in aquatic environments usually does not exceed a few percent of the total bacterioplankton abundance [59]. According Gazol et al. [50], this is partly because the physiological activity of a bacterium is in direct proportion to its size, meaning that most of the UMB predominant in the bacterioplankton are dormant cells. However, the use of CTC as a marker of metabolic activity has serious disadvantages. First, CTC-positive ($^+$) cells are not always synonymous with 'growing cells' in that Bernard et al. [59] could find no correlation between them and bacterial production. Moreover, even a negative relationship has been observed between the growth rate and the amount of CTC fluorescence per cell [60]. Another methodological problem is that the smaller the respiring (CTC^+) cell, the smaller the formazan crystals that form in it, and therefore the weaker their fluorescence. As a result, it is more difficult to recognize CTC fluorescence in the smallest cells and, hence, the latter have a lower chance than the normal cells to be identified as active.

Nevertheless, let us assume that the empirical model in [50] is true when applied to our samples, namely that the probability (P, %) for a bacterial cell to be active (more strictly, CTC^+) is a function of its volume (V, μm^3) and can be calculated for the cell size range up to 0.28 μm^3 (larger cells are considered active) as: $P = 8.57 + 318.2 \times V$. Then it is possible to check to which extent the dormancy of the small bacteria can affect the results. Approximations were made for the 7 samples presented in Fig. 3A–G to determine the fractions of the active cells in the total bacterial abundance, biovolume and biosurface in Fig. 7A. Confidence intervals (CI) were calculated from 100 randomized runs ($0 \le p \le 1$) made for each of the 50 sized cells in every sample to determine the cell physiological status (active at $p \le P$, otherwise inactive). The curves were parallel with the highest percentage that of the active biovolume and the lowest one that of cell abundance. A half of the small (<0.2 μm^3) bacteria were inactive while their contribution to the total biosurface and, especially, to the biovolume was much less in total. Hence, the model must have the largest effect on the cell-specific flux and the smallest one on the biovolume-specific flux. The latter is the principal factor in the on-going debate on the physiological status of the smallest planktonic bacteria and coincidentally that is why the same approximations were made for the data in Fig. 6E. The results presented in Fig. 7B showed that the dormancy of the small cells does not change the situation. The volume-specific fluxes were higher for smaller cells because they were calculated per active cells only, but the dependence remained weak ($r^2 = 0.16$) due to the high variability (over 2 orders of magnitude) of the energy flux in the natural community. Thus, the occurrence of a large sub-population of dormant cells in the

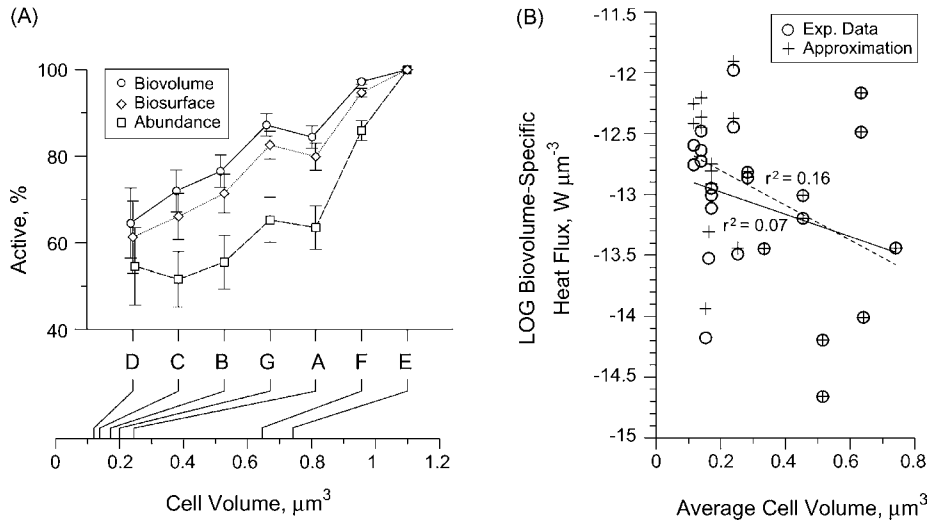

Fig. 7. (A) Percentage of the active cells in terms of their abundance, biovolume and biosurface, approximated for the samples A–G (see Fig. 3) according to [50]. The values are the mean ± 95% CI. (B) Biovolume-specific energy fluxes measured for the picoplankton community (◯) and their approximations for the metabolically active cells (+) according to [50].

smallest bacterioplankton means at the same time that the other live sub-population must be highly active per cell volume, even more so than the 'normal' bacteria in the picoplankton. The paradox of the two opposite hypotheses for the physiological status of living UMB, namely dormant or metabolically active, are reconciled in this context to produce the following suggestion: A bacterial cell that is in the femtoplankton (<0.2 μm) has to have either the lowest or the highest volume-specific metabolic rate; the middle rates are rather for 'normal' bacterioplankton.

Recently, it has been realized that a large fraction of bacteria in marine environments are dead cells, up to 80% according to [61] and our data on bacterioplankton in Sevastopol Bay (Lopukhina, Mukhanov and Kemp, unpublished). However, there are no data on whether or not bacterial viability depends on the cell size. If not, there would be no effect on the lack of dependence of the fluxes on the average cell size, except that all the fluxes calculated per live abundance, biovolume and biosurface would be higher in proportion.

More than 99% of the planktonic bacteria able to survive in nutrient-depleted pelagic environments cannot be isolated to a culture using standard nutrient-rich media [40,62]. Unfortunately, this excludes them from the list of the microbial species for which experiments can be devised to test the applicability of the conventional allometric rules. Not all planktonic microorganisms though are in this situation. In particular, Caron et al. [63] demonstrated a perfect ($r^2 = 0.78$) allometric dependence of the cell volume-specific respiration rate on the cell volume (over 6 orders of magnitude, 10^2–10^8 μm^3) with the exponent of $-1/3$ ($b = 2/3$ in the original form of the Kleiber equation [42], $R = a \times W^b$, where R is the metabolic rate, W is the organism mass) for a wide range of culturable aquatic protozoans actively growing under favourable conditions. We converted these data to the 'per cell surface' basis and obtained a perfect fit to Rubner's law [64], i.e. the complete lack ($r^2 < 0.001$) of size-dependence for the oxygen flux of the protozoa (Fig. 8, inset symbols 5–7).

It is important to note that natural populations grow more slowly so, if the data for them were to be added to the plot, the points would lie below the horizontal regression line obtained for the active growth (Fig. 8). In explaining this result, it is important to recall that the uptake of nutrients and co-factors across the cell surface is governed by Fick's first law of diffusion, which is a passive process and active transport by plasma membrane permeases that require cell energy (ATP). In oligotrophic environments, the concentrations of metabolites in the water column are low and thus, according to Fick's law, their rate of passive transport would be slow. Permeases increase nutrient uptake against the concentration gradient but in conditions of low concentration there is a limit to how much can be taken up so it is reasonable to suppose that the number of transporters would be small to avoid redundancy. On this tentative hypothesis, obligate

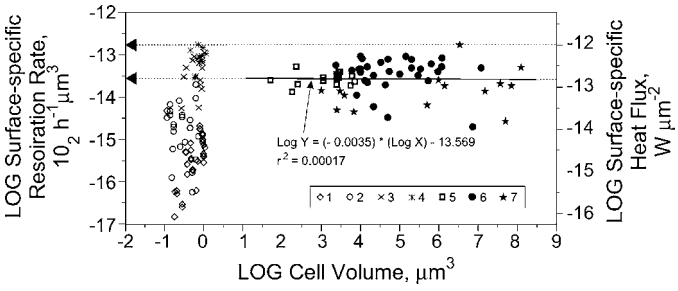

Fig. 8. Dependence of biosurface-specific metabolic rate on cell size in aquatic unicellular microorganisms. The inset denotes the source of the data described as follows. Our data for the picoplankton enrichment culture aging for 15 weeks (1) and the coastal and mesocosm picoplankton (2). 24-h bacterial growth [65] of *Escherichia coli* (3) in 1% peptone and in peptone + 0.5% glucose media; and of *Salmonella pullorum* (4) in 1% peptone medium. Data for aquatic protozoans approximated from those in a review by Caron et al. [63]: actively growing flagellates (5), ciliates (6) and sarcodines (7). The regression line obtained for the protozoans corresponds to the oxygen flux of 3.6×10^{-14} l O_2 h^{-1} μm^{-2} (bottom arrow). The upper limit of the flux (top arrow) is about 17.2×10^{-14} l O_2 h^{-1} μm^{-2}. The oxygen (left axis) and heat (right axis) fluxes are converted to each other assuming an oxycaloric equivalent of -450 kJ mol^{-1} O_2 [12].

oligotrophs from the UBM pool cannot respond to higher nutrient concentrations because they do not have enough transporters. By modifying Rubner's idea, it is logical to suggest that the metabolic rate of oligobacteria suspended in the water column is limited by the permease-mediated rate of transport of metabolites across their surface membranes. Applying this to the whole community means that there is a limitation of the overall energy flow through it by the transport of metabolites through its biosurface. Thus, there must be a maximum rate of transport which corresponds to the maximum biosurface-specific metabolic flux.

For the data on protozoans, two values (or constants) of the surface-specific metabolic flux can be recognized as the highest limits. The first one, an average calculated for the data in Fig. 8 (symbols 5–7), is 3×10^{-14} l O_2 μm^{-2} h^{-1}, or about 2×10^{-13} W μm^{-2} in terms of heat flux at the oxycaloric equivalent averaged for all small carbon compounds of -450 kJ mol^{-1} O_2 [12]. The second constant is the highest flux registered which is about 10^{-12} W μm^{-2} for the sarcodines. The data provided for the picoplankton (Fig. 8, symbols 1 and 2) are below the first constant, with the highest values approaching the constant obtained for the natural community, not for the culture. Actively growing bacteria can exhibit higher fluxes though, as seen in the symbols 3 and 4 in Fig. 8. To illustrate this, we involved the results obtained by Huntington and Winslow [65] in a pioneering study of the dynamics of the cell volume-specific metabolic rates during the early phases of growth of two bacterial cultures. The rates of carbon dioxide production provided by the authors were converted to oxygen uptake rates assuming a respiratory quotient of 1. Most of the points are above the first flux constant (Fig. 8). It is notable that the highest values proved to fit the second flux constant, 1 pW μm^{-2} (Fig. 8, symbol 4 for *S. pullorum*).

The above constant can have an ecological sense, though more data are needed to check on the regularity of it. Biosurface-specific fluxes measured in a natural assemblage per the total (using acridine orange or DAPI direct counts and sizing) and intact (using e.g. propidium iodide) biosurfaces can be compared with it and their ratio can be calculated to estimate the *efficiency* of the material and energy flow through the community biosurface. In bacterioplankton, this index appears not to exceed 5–10% [9,10].

5. Conclusions

1. About a 6-fold reduction in bacterial size over the 15-week period of senescence of the enriched heterotrophic picoplankton was associated with a more than 2 orders of magnitude decrease in the bacterial heat fluxes calculated per total cell abundance without a distinction between dead/alive and active/dormant cells.
2. The heat fluxes measured for the aging culture of heterotrophic picoplankton never exceeded and were usually lower than those for the natural assemblage.
3. In the natural assemblage, the biovolume-specific heat fluxes insignificantly increased with decreasing average cell size. The lack of dependence was probably due to the structural complexity of the natural community (multispecies system, different cell morphotypes and physiological states). When taken together with the empirical model by Gazol et al. [50] showing that most UMB are dormant, this result provided evidence that there can be in fact two sub-populations of them in terms of physiological activity, with the extremely low (dormant forms of copiotrophs) and extremely high (probably, oligobacteria) volume-specific metabolic rates.
4. The maximum biosurface-specific metabolic rate measured for the natural bacteria was close to that averaged for actively growing aquatic protozoans. The latter is independent of the cell volume over the size range from the smallest flagellate to the largest sarcodines, supplying illustrative evidence for Rubner's law. Marine bacteria appear to fit this law and extend its scale by 2 orders of magnitude.
5. It is suggested that the highest biosurface-specific energy flux in heterotrophic picoplankton is limited by the permease-mediated rate of transport of metabolites across the plasma membrane. If the suggestion is correct, the upper limit of the flux has an ecological meaning, characterising the *efficiency* of the material and energy flows through the community biosurface.

Acknowledgements

The study was funded by EC INTAS grants 99-0139 and 03-51-6196.

References

[1] W. Whitman, D. Coleman, W. Wiebe, Proc. Nat. Acad. Sci. USA 95 (1998) 6578–6583.
[2] P.G. Falkowski, R.T. Barber, V. Smetacek, Science 281 (1998) 200–206.
[3] F. Azam, T. Fenchel, J.G. Field, J.S. Gray, L.A. Mayer–Reil, F. Thingstad, Mar. Ecol. Prog. Ser. 10 (1983) 257–263.
[4] T. Fenchel, Adv. Microb. Ecol. 9 (1986) 57–97.
[5] D.A. Caron, E.L. Lim, G. Miceli, J.B. Waterbury, F.W. Valois, Mar. Ecol. Prog. Ser. 76 (1991) 205–217.
[6] R.B. Kemp, in: E.E. Bittar, N. Bittar (Eds.), Principles of Medical Biology, vol. 4 (Part 111), JAI Press, Greenwich, USA, 1996, pp. 303–329.
[7] J.A. Runge, M.D. Ohman, Limnol. Oceanogr. 27 (1982) 570–576.
[8] I.R. Joint, A.J. Pomeroy, Mar. Biol. 77 (1983) 19–27.
[9] V.S. Mukhanov, O.A. Rylkova, O.A. Lopukhina, R.B. Kemp, Thermochim. Acta 397 (2003) 31–35.
[10] V.S. Mukhanov, O.G. Naidanova, N. Shadrin, R.B. Kemp, Aquat. Ecol. 38 (2004) 375–385.
[11] V.S. Mukhanov, R.B. Kemp, Mar. Ecol. J. Special vol.1 (2005) 84–98.
[12] E. Gnaiger, R.B. Kemp, Biochim. Biophys. Acta 1016 (1990) 328–332.
[13] E.H. Battley, Energetics of Microbial Growth, John Wiley & Sons Inc., New York, 1987.
[14] B. Larsson, L. Gustafsson, in: R.B. Kemp (Ed.), Handbook of Thermal Analysis and Calorimetry, vol.4, Elsevier, Amsterdam, 1999, pp. 367–404.
[15] M.M. Pamatmat, Mar. Biol. 129 (1997) 735–746.
[16] M.M. Pamatmat, J. Plankton Res. 25 (2003) 461–464.
[17] M.H. Howard–Jones, M.E. Frischer, P.G. Verity, in: J.H. Paul (Ed.), Methods in Microbiology, vol.30, Academic Press Ltd., San Diego, 2001, pp. 175–206.
[18] G.G. Rodriguez, D. Phipps, K. Ishiguro, H.F. Ridgway, Appl. Environ. Microbiol. 58 (1992) 1801–1808.
[19] E.M. Smith, Aquat. Microb. Ecol. 16 (1998) 27–35.
[20] T. Nyström, Ann. Rev. Microbiol. 58 (2004) 161–181.
[21] S.E. Finkel, Nature Rev. Microbiol. 4 (2006) 113–120.
[22] E. Zinser, R. Kolter, J. Bacteriol. 181 (1999) 5800–5807.

[23] E. Zinser, R. Kolter, Res. Microbiol. 155 (2004) 328–336.
[24] L.W. Haas, Ann. Inst. Oceanogr. (Paris) 58 (1982) 261–266.
[25] A.G. Rodina, Methods in Aquatic Microbiology, University Park Press, Baltimore, Maryland, USA, 1972, 461p.
[26] G. Bratbak, in: P.F. Kemp, B.F. Sherr, J.J. Cole (Eds.), Handbook of Methods in Aquatic Microbial Ecology, Lewis Publishers, Boca Raton, 1993, pp. 309–318.
[27] B. Sherr, E. Sherr, P. del Giorgio, in: J.H. Paul (Ed.), Methods in Microbiology. Marine Microbiology, Academic Press, San Diego, 2001, pp. 129–160.
[28] D.L. Kirchman, in: P.F. Kemp, B.F. Sherr, E.B. Sherr, J.J. Cole (Eds.), Handbook of Methods in Aquatic Microbial Ecology, Lewis Publishers, Boca Raton, 1993, pp. 117–120.
[29] H. Eilers, J. Pernthaler, R. Amann, Appl. Environ. Microbiol. 66 (2000) 4634–4640.
[30] A. Pernthaler, J. Pernthaler, H. Eilers, R. Amann, Appl. Environ. Microbiol. 67 (2001) 4077–4083.
[31] A.J. Smigielski, Respiration and other physiological characteristics of relevance to dwarfing and survival in marine vibrios, Diss. Abst. Int. Pt. B. Sci. 51 (1991).
[32] D.K. Button, Appl. Environ. Microbiol. 57 (1991) 2033–2038.
[33] B. Velimirov, Microbes Environ. 16 (2001) 67–77.
[34] R. Kolter, D.A. Siegele, A. Tormo, Ann. Rev. Microbiol. 47 (1993) 855–874.
[35] S.E. Finkel, E. Zinser, R. Kolter, in: G. Storz, R. Hengge–Aronis (Eds.), Bacterial Stress Responses, ASM Press, Washington DC, 2000, pp. 231–238.
[36] S.E. Finkel, R. Kolter, Proc. Natl. Acad. Sci. USA 96 (1999) 4023–4027.
[37] E.A. Dawes, Symp. Soc. Gen. Microbiol. 26 (1976) 19–53.
[38] J.A. Novitsky, R.Y. Morita, Mar. Biol. 48 (1978) 289–295.
[39] G. Kurath, Y. Morita, Appl. Environ. Microbiol. 45 (1983) 1206–1211.
[40] D.B. Roszak, R.R. Colwell, Microbiol. Rev. 51 (1987) 365–379.
[41] A. Unge, R. Tombolini, L. Mølbak, J.K. Jansson, Appl. Environ. Microbiol. 65 (1999) 813–821.
[42] M. Kleiber, Hilgardia 6 (1932) 315–353.
[43] M. Kleiber, The Fire of Life: An Introduction to Animal Energetics, John Wiley and Sons, New York, USA, 1961, 454 p.
[44] A.M. Makarieva, V.G. Gorshkov, Bai–Lian Li, Proc. Royal Soc. Biol. Ser. 272 (2005) 2219–2224.
[45] S.P. Blight, T.L. Bentley, D. Lefevre, C. Robinson, R. Rodrigues, J. Rowlands, P.J.leB. Williams, Mar. Ecol. Progr. Ser. 128 (1995) 61–75.
[46] J.M. Sieburth, V. Smetacek, J. Lenz, Limnol. Oceanogr. 23 (1978) 1256–1267.
[47] A.L. Koch, Ann. Rev. Microbiol. 50 (1997) 317–348.
[48] J. Maniloff, K.H. Nealson, R. Psenner, M. Loferer, R.L. Folk, Science 276 (1997) 1776.
[49] F. Schut, R.A. Prins, J.C. Gottschal, Aquatic Microb. Ecol. 12 (1997) 177–202.
[50] J.M. Gazol, P.A. del Giorgio, R. Massana, C.M. Duarte, Mar. Ecol. Prog. Ser. 128 (1995) 91–97.
[51] D.K. Button, B.R. Robertson, Cytometry 10 (1989) 558–563.
[52] W.K. Li, P.M. Dickie, Mar. Ecol. Prog. Ser. 26 (1985) 245–252.
[53] T. Nyström, P. Marden, S. Kjelleberg, FEMS Microb. Ecol. 38 (1986) 285–292.
[54] L.H. Stevenson, Microb. Ecol. 4 (1978) 127–133.
[55] A.F. Carlucci, S.L. Shimp, D.B. Craven, FEMS Microb. Ecol. 45 (1987) 211–220.
[56] F. Schut, E.J. de Vries, J.C. Gottschal, B.R. Robertson, W. Harder, R.A. Prins, D.K. Button, Appl. Environ. Microbiol. 59 (1993) 2150–2160.
[57] J.A. Fuhrman, Mar. Ecol. Prog. Ser. 5 (1981) 103–106.
[58] S. Lee, J.A. Fuhrman, Appl. Environ. Microbiol. 53 (1987) 1298–1303.
[59] L. Bernard, C. Courties, P. Servais, M. Trousselier, M. Petit, P. Lebaron, Microb. Ecol. 40 (2000) 148–158.
[60] M.E. Sieraci, T.L. Cucci, J. Nicinski, Appl. Environ. Microbiol. 65 (1999) 2409–2417.
[61] G.M. Luna, E. Manini, R. Danovaro, Appl. Environ. Microbiol. 68 (2002) 3509–3513.
[62] M. Eguchi, Y. Ishida, FEMS Microb. Ecol. 73 (1990) 23–30.
[63] D.A. Caron, J.C. Goldman, T. Fenchel, in: G.M. Capriulo (Ed.), Ecology of Marine Protozoa, Oxford University Press, Oxford, UK, 1990, pp. 307–322.
[64] M. Rubner, Z. Biol. 19 (1883) 535–562.
[65] E. Huntington, C.-E.A. Winslow, J. Bacteriol. 33 (1936) 123–144.